Bull. Chem. Soc. Jpn., ***74***, *245–254 (2001)* 245

Structures and Reactions of Alkoxymethyl(alkali metals). Ethylation by Methyl Ethers in the Presence of Organometallic Bases

Yuji Naruse, Akihiro Hayashi, Shin-ichiro Sou, Hirotaka Ikeda, and Satoshi Inagaki*

Department of Chemistry, Gifu University 1-1, Yanagido, Gifu 501-1193

(Received June 22, 2000)

Structures and reactions of CH_3OCH_2M (M = Li, Na, K) were investigated in a theoretical manner. CH_3OCH_2M has the acute bond angle of $\angle$M–C–O due to a strong coordination of the oxygen to the alkali metals. The nucleophilic substitution reaction of the substrate CH_3OCH_2Li by the nucleophile CH_3OCH_2Li is more preferred than the carbene generation by α-elimination and a nucleophilic substitution of CH_3OCH_2Li by CH_3Li. The resulting 2-methoxyethyllithium readily liberated lithium methoxide to afford ethylene, which added to the anion species to give an ethylated product. Among the CH_3OCH_2M (M = Li, Na, K), CH_3OCH_2K is the most nucleophilic, due to the high $\sigma_{C\text{–}K}$ level, while CH_3OCH_2Li is the most nucleophilic because of the lowest $\sigma^*_{C\text{–}O}$ level. This supports a previously proposed mechanism for the ethylation of indole derivatives by methyl ethers in the presence of BuLi - *t*-BuOK.

Recently, we have reported the ethylation of indole dianions by methyl ethers[1] in the presence of the superbase, BuLi–*t*-BuOK[2] (Eq. 1). In our case, the ethylated product was obtained predominantly and indoles with longer alkyl side chains were obtained only in small amounts. Ziegler, however, reported that butyllithium reacts with dimethyl ether to give a mixture of pentane, hexane, heptane and octane.[3] These products were supposed to come from sequential insertions of methoxymethyllithium or carbene, generated *in situ* from dimethyl ether, to the alkyllithium. These two results sharply contrast with each other.

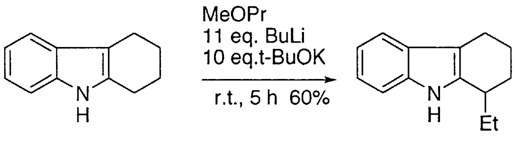

(1)

Here, we studied the structures and reactions of methoxymethyl(alkali metals) as a prototype of the intermediate generated from methyl ethers in the presence of organometallic bases. We also investigated subsequent reactions of the products and related reactions to explore the mechanism of ethylation by methyl ethers in the presence of organometallic bases, especially to understand the preferred ethylation and the role of the superbase.

Method of Calculation

We proposed and applied a bond model to analyze the electronic structures of molecules[4–8] and transition states.[9] The single Slater determinant of the Hartree–Fock wave function (Ψ) for the electronic structure of the molecule or the transition state can be expanded into electron configurations,[6]

$$\Psi = C_G\Phi_G + \sum C_T\Phi_T + \sum C_E\Phi_E + ...$$

In the ground configuration (Φ_G), a pair of electrons occupies each bonding orbital of the bonds. A ground configuration corresponds to a Lewis structure for an electronic formula of a molecule to show the location of valence electrons. The interactions between the bond orbitals are accompanied by electron delocalization and polarization. The delocalization is expressed by mixing an electron-transferred configuration (Φ_T), where an electron shifts from the bonding orbital of a bond to the antibonding orbital of another. The polarization is expressed by mixing a locally excited configuration (Φ_E) where an electron is promoted from the bonding orbital to the antibonding orbital of a bond.

A set of bond orbitals, i.e., hybrid orbitals and bond polarities (BPL) $|c_{ia}/c_{ib}|$,[10] gives the coefficients of the configurations (C_G, C_T, and C_E). The bonding and antibonding orbitals (ϕ_i and $\phi_i{}^*$) of the *i*th bond are expressed by a linear combination of the hybrid atomic orbitals (χ_{ia} and χ_{ib}) on the bonded atoms (a and b):

$$\phi_i = c_{ia}\chi_{ia} + c_{ib}\chi_{ib},$$

$$\phi_i{}^* = c_{\mathrm{ia}}{}^*\chi_{\mathrm{ia}} + c_{\mathrm{ib}}{}^*\chi_{\mathrm{ib}}.$$

The bond (bonding and antibonding) orbitals of each bond are obtained by diagonalization of the 2 × 2 Fock matrix on the basis of hybrid orbitals.[10] A set of bond orbitals are optimized[6,10] to give the maximum value of the coefficient of the ground configuration.

There can be some Lewis structures for the molecules or the transition states. Which Lewis structure best represents the electron states is determined by the Lewis index[4] (C_G) , a measure of the contribution from the Lewis structure to the total electronic structure. We chose the bond model of the greatest Lewis index to investigate the bond interactions. The delocalization index is defined as the relative ratio of the coefficient of the transferred configuration to that of the ground configuration ($|C_T/C_G|$)[5] to estimate the delocalizability between the bonds. In order to estimate the interaction of the bond orbitals (i and j) we calculated the interbond energy IBE(i,j),[7]

$$\mathrm{IBE}_{(i,j)} = P_{ij}(\mathrm{H}_{ij} + F_{ij}),$$

where P_{ij}, F_{ij}, and H_{ij} are the elements of the density, Fock, and core Hamiltonian matrices, respectively.

Geometry optimization of molecules and transition states[11] was conducted throughout this paper by *ab initio* molecular orbital calculations at the RHF/6-31G* level using the GAUSSIAN 98 program.[12] All geometries examined here were checked by frequency calculations, and the located transition state geometries were subjetcted to the IRC calculations for a confirmation. The thus-obtained wave functions at the RHF/6-31G* level were employed for bond model analyses. The contour maps of the orbitals were drawn by the MOPLOT program.[13]

Results and Discussions

Structures of CH_3OCH_2M (M = Li, Na, K). We optimized the structure of CH_3OCH_2M (M = Li, Na, K).[14] The results of the calculations showed an interesting geometrical feature. The bond angles ∠MCO are acute (Fig. 1). This peculiar feature suggests that the C–M bonds are not simply the usual ionic bonds. We thus investigated the chemical bonding in CH_3OCH_2M. Possible bond structures are represented by the σ bond model (**i**), the ylide model (**ii**), the ionic bond model (**iii**), the carbene complex model (**iv**), and the divalent metal complex (**v**) in Fig. 2. The highest values of the Lewis indices (Table 1) were obtained for the σ bond models irrespective of the metals. A remarkable difference of M = K was found from M = Li and Na. The (relative) Lewis indices of the ylide, ionic bond and carbene complex structures are appreciably high for M = K.

We investigated the bond interactions in the σ bond model. The acute angle of Li–C–O (61.2°) was found to come from a strong coordination of the oxygen atom to the Lewis acidic lithium, which shortens the distance between Li and O (Total of $\mathrm{IBE}_{(\mathrm{n\text{-}p^*Li})} = -0.978$ a.u.). The sodium and potassium analogs have acute bond angles (67.2° and 67.8°, respectively), while the coordinations are weakened (IBE's = -0.645 and -0.399 a.u., respectively).

The electronic structures around the metallated carbon are significant to the reactions. The most electron-donating bonds are the C–M bonds. The energy of the bonding orbitals increases in the order $\sigma_{\mathrm{C-Li}} < \sigma_{\mathrm{C-Na}} < \sigma_{\mathrm{C-K}}$ (Table 2), as is expected from the ionization potentials of the metals. The energy order suggests that the potassium intermediate is the most powerful donor. The bonding orbital extension appreciably deviates from the C–M bond axis outwards (for example, see the case M = Li in Fig. 3). The most electron-accepting bond orbitals around the reactive center are the antibonding orbitals of the bonds between the oxygen atom and the metallated carbon. The $\sigma^*_{\mathrm{C-O}}$ energy also increases in the same order, suggesting that the lithium derivative is the most powerful electron accep-

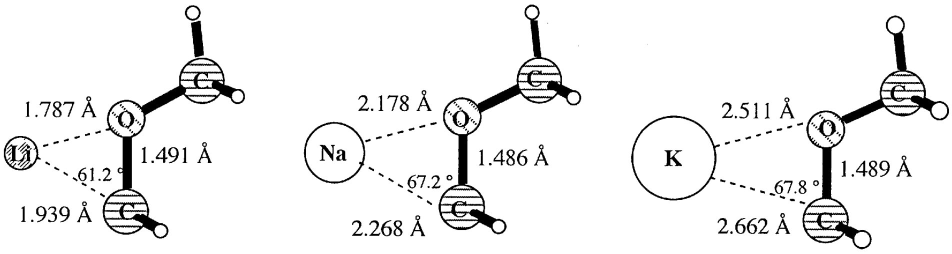

Fig. 1. Structures of CH_3OCH_2M.

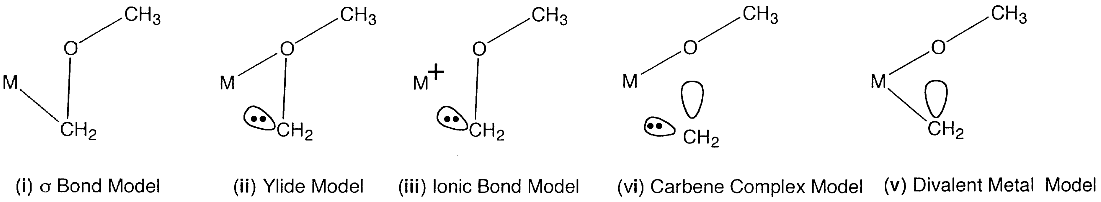

(i) σ Bond Model (ii) Ylide Model (iii) Ionic Bond Model (vi) Carbene Complex Model (v) Divalent Metal Model

Fig. 2. Bond models of CH_3OCH_2M (M = Li, Na, K).

Table 1. Lewis Index

	Bond Model				
M	σ Bond	Ylide	Ionic bond	Carbene complex	Divalent metal
Li	1.634	1.181	1.062	0.736	1.127
Na	1.701	1.289	1.199	0.782	1.072
K	1.723	1.426	1.365	0.869	1.089

Table 2. Electronic Features of CH_3OCH_2M (M = Li, Na, K)

	Bond Orbital Energy/a.u.			
M	σ_{C-M}	σ^*_{C-O}	Charges[a)]	C–M Bond Polarity[b)]
Li	−0.653	0.627	−0.280	4.47
Na	−0.538	0.663	−0.345	4.63
K	−0.510	0.686	−0.392	5.54

a) Total atomic charges on the metallated carbon. b) See the definition in the text.

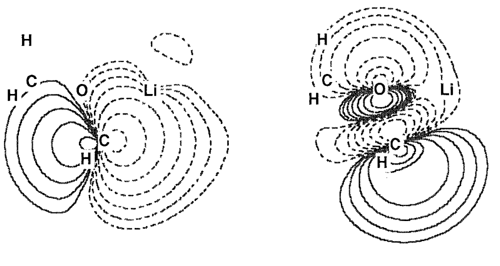

(A) (B)

Fig. 3. σ_{C-Li} (A) and σ^*_{C-O} (B) of CH_3OCH_2Li.

tor. The ordering possibly results from the negative charge on the metallated carbons, as expected from the C–M bond polarity (Table 2). The antibonding orbitals extend on the C–O bond as usual.

Reactions of CH_3OCH_2M. We investigated some reactions of the first intermediate CH_3OCH_2M generated during the ethylation by methyl ethers in the presence of organometallic bases (Scheme 1).[15] Among them are included (a) methylene transfer from one molecule to another to produce $CH_3OCH_2CH_2M$ (Eq. 2), (b) methylene transfer to CH_3M as a model reaction of the sequential methylation of the carbanion (Eq. 3), and (c) α-elimination to generate methylene (Eq. 4), which dimerizes into ethylene. We also investigated the subsequent reactions of the intermediates generated by the preceding reactions to fully understand the ethylation reaction. The elementary reaction examined here are: (d) β-elimination of $CH_3OCH_2CH_2Li$ to generate ethylene (Eq. 5); (e) insertion of ethylene into the C–Li bond of the substrate CH_3Li or nucleophilic addition of CH_3Li to ethylene (Eq. 6).

$$2\,CH_3OCH_2M \xrightarrow[-\,CH_3OM]{} CH_3OCH_2CH_2M \quad (2)$$

$$CH_3M + CH_3OCH_2M \xrightarrow[-\,CH_3OM]{} CH_3CH_2M \quad (3)$$

$$CH_3OCH_2M \xrightarrow[-\,CH_3OM]{} :CH_2 \quad (4)$$

$$CH_3OCH_2CH_2M \xrightarrow[-\,CH_3OM]{} H_2C{=}CH_2 \quad (5)$$

$$CH_3M + H_2C{=}CH_2 \longrightarrow CH_3CH_2CH_2M \quad (6)$$

Methylene Transfer between CH_3OCH_2M's. We studied the C_2 unit formation from two molecules of CH_3OCH_2Li (Eq. 2). A transition structure (Fig. 4) was located for this elementary reaction of the C–C bond formation between two molecules of CH_3OCH_2Li. The distance of the incipient bond between the carbons is somewhat long (2.594 Å). We performed IRC calculations to confirm that the final points led to the reactant and the product. The optimized structures at the stationary points are shown in Fig. 5 together with the relative energies. The two molecules of CH_3OCH_2Li initially form the in-line bimolecular complex, which is more stable by 10.2 kcal mol^{-1}. The activation energy is 27.5 kcal mol^{-1} from the complex. The geometry of the molecule which accepts the methylene remains almost unchanged from that in the isolated state. On the other hand, the C–O bond is remarkably elongated in the molecule donating the methylene. The structure indicated a transfer

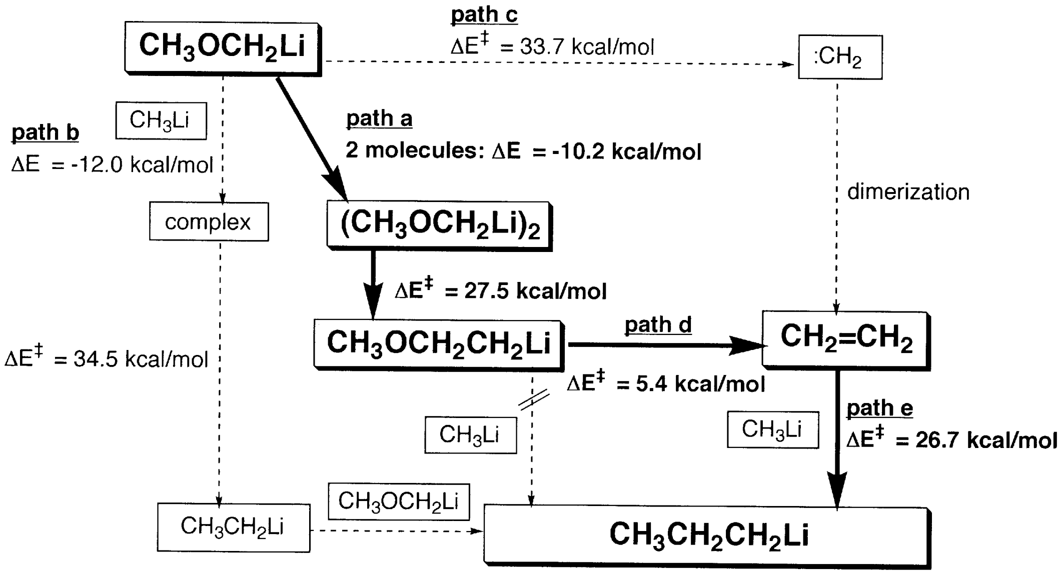

Scheme 1.

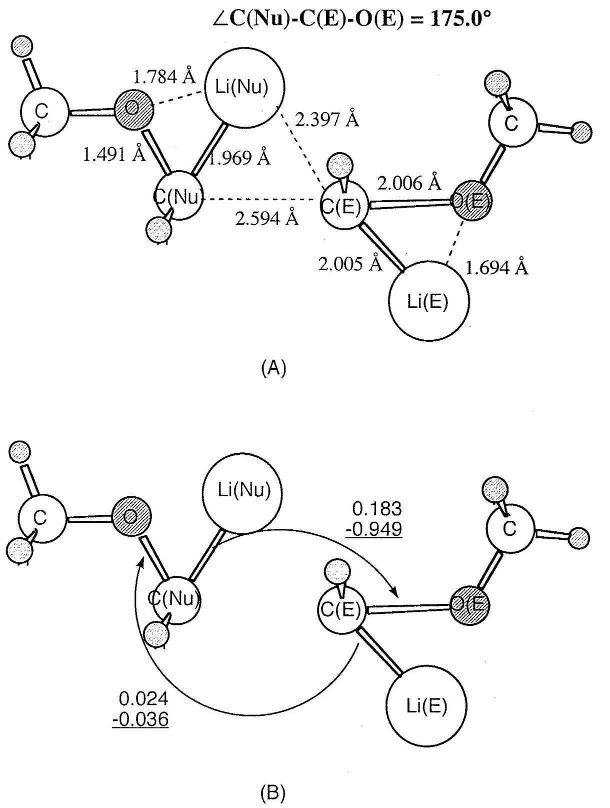

Fig. 4. Transition structure (A) and the delocalization indices and IBE values (underlined) (B) of the methylene transfer between two molecules of CH_3OCH_2Li.

of the methylene group from one molecule to the other. To probe the characteristic feature of this reaction, we analyzed the bond interaction at the transition state. We employed the σ bond model for the reactants, which has been found to have the highest Lewis index. The most stabilizing bond interaction occurs between $\sigma_{\text{C-Li/Nu}}$ of one molecule and $\sigma^*_{\text{C-O/E}}$ of the other (IBE($\sigma_{\text{C-Li/Nu}} - \sigma^*_{\text{C-O/E}}$) = – 0.949, Delocalization index 0.183), while the reverse delocalization from $\sigma_{\text{C-Li/E}}$ to $\sigma^*_{\text{C-O/Nu}}$ is small IBE ($\sigma_{\text{C-Li/E}} - \sigma^*_{\text{C-O/Nu}}$) = – 0.036, Delocalization index 0.024). This is a characteristic feature of the nucleophilic substitution. One molecule acts as a nucleophile, while the other molecule acts as an electrophile. The substitution occurs at the methylene carbon. The nucleophilic center is the carbon atom bonded to Li. The leaving group is the methoxy group. The nucleophilic center reacts in retaining the configuration, and the electrophile inverts the configuration. At the transition structure the three atoms of C(Nu)–C(E)–O(E) locate almost in a line (∠C(Nu)–C(E)–O(E) = 175°). Two molecules exist in unsymmetrical positions to favor the overlap between the bonding orbital of the $\sigma_{\text{C-Li}}$ bond in the nucleophilic molecule and the antibonding orbital of the $\sigma_{\text{C-O}}$ bond in the electrophilic molecule, as shown in Fig. 6. The methylene transfer reaction is closely related to the Si–Si bond formation reaction of two molecules of alkoxysilyllithium, recently reported by Tamao and Nakatsuji.[16]

The reactant molecules CH_3OCH_2Li were shown to play opposite donor–acceptor parts. This led to an interesting prediction of the effects of alkali metals (M = Li, Na, K) on the reactivities. As we have shown, heavier alkali metals increase the $\sigma_{\text{C-M}}$ orbital energy level to enhance the capability as donors. Lighter metals lower the $\sigma^*_{\text{C-O}}$ orbital energy level to enhance the capability as acceptors. The most reactive pairs of the reactants are predicted to be CH_3OCH_2K as a nucleophile and CH_3OCH_2Li as a substrate (electrophile). The prediction was confirmed by the calculated activation energies (Tables 3 and 4).

Methylene Transfer from CH_3OCH_2Li to CH_3Li. Ethylation by methyl ethers in the presence of organometallic bases may involve a sequential transfer of the methylene group

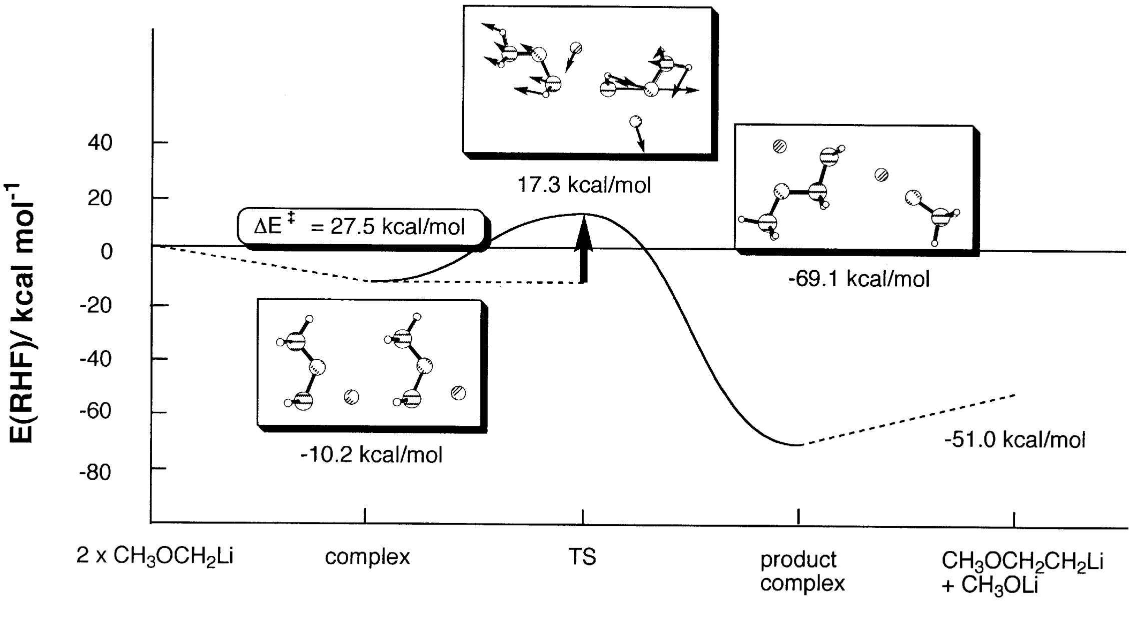

Fig. 5. Reaction profile of CH_3OCH_2Li + CH_3OCH_2Li.

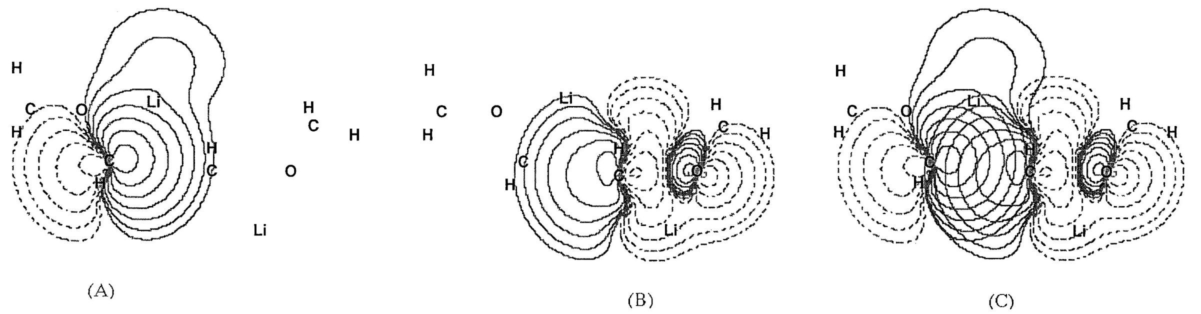

Fig. 6. σ_{C-Li} of the nucleophile (A), σ^*_{C-O} of the electropohile (B), and both orbitals superimposed (C) at the transition statte of the methylene transfer between two molecules of CH_3OCH_2Li.

Table 3. Calculated Activation Energies of the Methylene Transfer Reactions between Two Molecules of CH_3OCH_2M (ZPE corrected)

M^1(nucleophile)	M^2(electrophile)	$\Delta E^{\ddagger}$/kcal mol^{-1}
Li	Li	27.6
Na	Li	25.8
K	Li	22.4
Li	Na	33.0
Li	K	36.1

Table 4. Energy Levels (in a.u.) of the Bond Orbitals σ_{C-Li} and σ^*_{C-X} (X = O, N, S)

X	$F(\sigma_{C-Li})$	$F(\sigma^*_{C-X})$	$\Delta\,|\,E\,|$
O	−0.6530	0.6259	1.2789
N	−0.6559	0.6974	1.3533
S	−0.7541	0.3109	1.0650

from CH_3OCH_2M to the metallated carbon atom of the substrate (Eq. 3). We located a transition structure (Fig. 7) where CH_3Li was employed as a model substrate. The reaction profile is shown in Fig. 8. In this reaction, the complex was initially formed. The complexation energy was – 12.0 kcal mol^{-1}. The reaction barrier from the complex (34.5 kcal mol^{-1}) was found to be higher by 7.0 kcal mol^{-1} than that of the methylene transfer between CH_3OCH_2Li (27.5 kcal mol^{-1}). We can rule out sequential methylene transfer. The reaction is also a nucleophilic substitution, just like the methylene transfer between CH_3OCH_2Li's. The nucleophilic center reacts in the retention of the configuration, and the electrophile inverts its configuration. The three atoms C–C–O locate exactly in a line (∠C–C–O = 180.0°). The breaking C–O bond length is slightly longer than that at the transition structure of the methylene transfer between two molecules. The incipient C–C bond is slightly shorter. The bond lengths suggest a later transition state, in agreement with the Hammond postulate.

The nucleophile CH_3Li might be more powerful than nucleophile CH_3OCH_2Li in the methylene transfer reactions between two molecules of CH_3OCH_2Li, since the σ_{C-Li} orbital level of CH_3OCH_2Li is lowered by electron-negative oxygen. In fact, the σ_{C-Li} orbital energies (– 0.634 a.u.) of the CH_3Li are higher than those of CH_3OCH_2Li (– 0.876 a.u.). However, the C–Li orbital of CH_3Li extends on the bond axis (Fig. 9); the overlap (0.472) with the σ^*_{C-O} at the transition state is less effective than that (0.949) of CH_3OCH_2Li, which has bent σ_{C-Li} (Fig. 6). The absence of a bent σ_{C-Li} bond was considered to be responsible for the high reaction barrier of the methylene transfer from CH_3OCH_2Li to CH_3Li, or the sequential methylene transfer reaction.

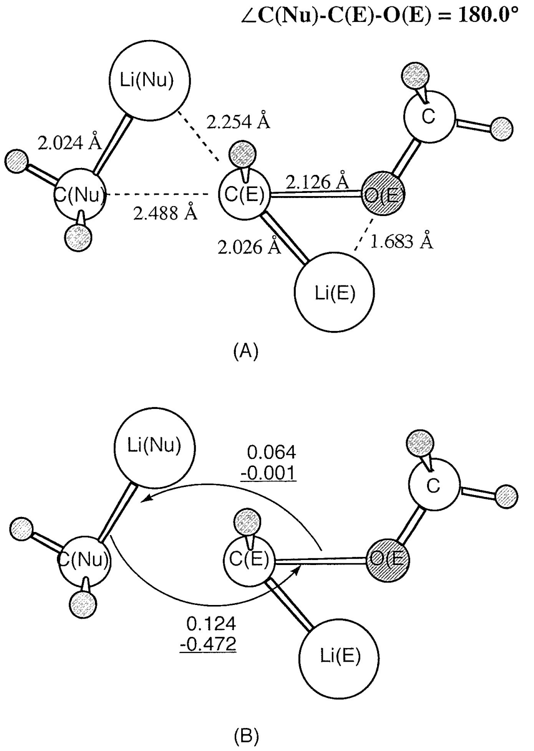

Fig. 7. Transition structure (A) and the delocalization indices and IBE values (underlined) (B) of the methylene transfer from CH_3OCH_2Li to CH_3Li.

Methylene Generation from CH_3OCH_2Li. We examined the first step of another possible reaction pathway of the ethylation by methyl ethers in the presence of organometallic bases, or the methylene (carbene) generation by the α-elimination reaction of CH_3OCH_2Li, which may be followed by dimerization into ethylene and the subsequent addition of ethylene to the substrate carbanions (Eq. 4). The transition structure (Fig. 10) has the highest Lewis index (Fig. 11) for the divalent metal model (1.397). The activation energy was found to

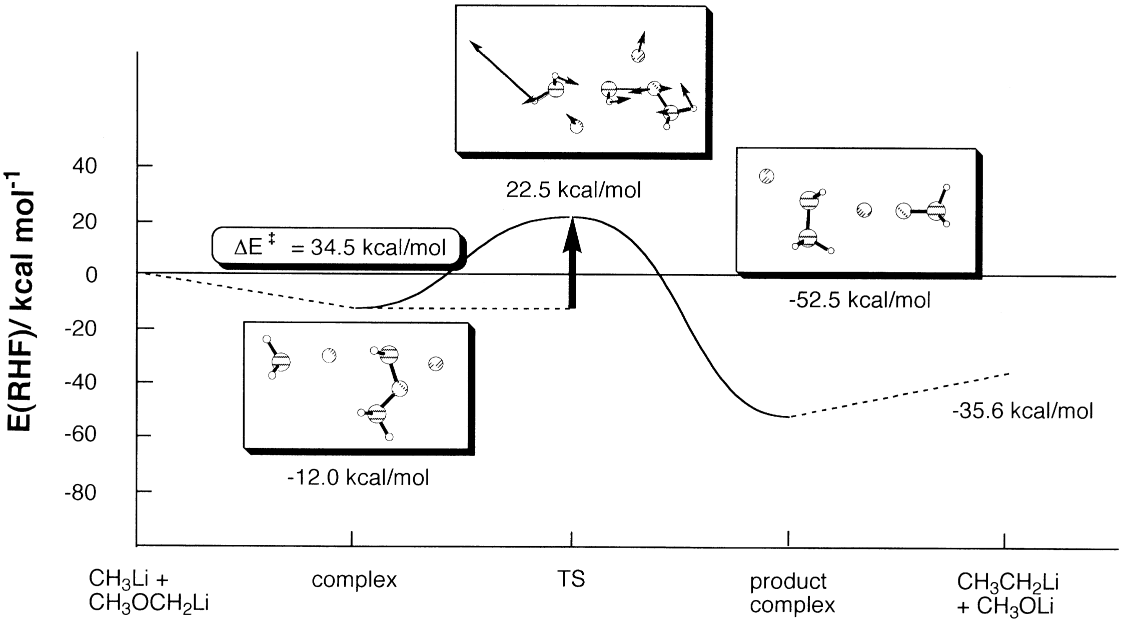

Fig. 8. Reaction profile of $CH_3Li + CH_3OCH_2Li$.

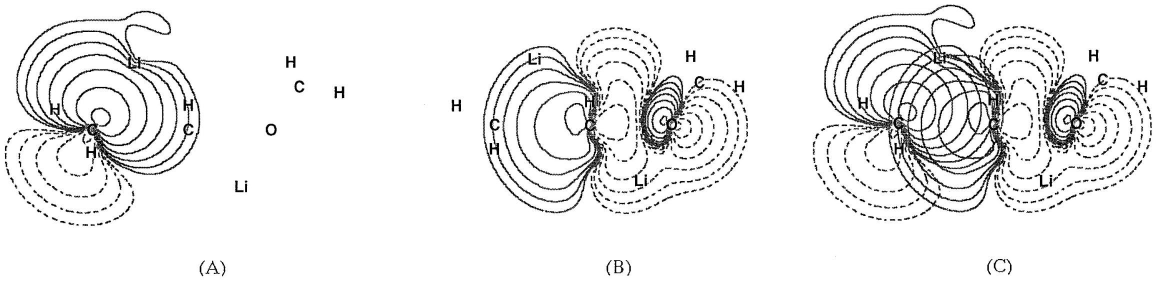

Fig. 9. σ_{C-Li} of CH_3Li (A), σ^*_{C-O} of CH_3OCH_2Li (B), and both orbitals superimposed at the transition state of the methylene transfer from CH_3OCH_2Li to CH_3Li.

be relatively high (33.7 kcal mol^{-1}). The barrier is higher than that for the methylene transfer between CH_3OCH_2Li by 6.2 kcal mol^{-1}. We can rule out the reaction pathway starting with the α-elimination of CH_3OCH_2M.

At the transition state, the carbene moiety does not appreciably interact with the other parts, except for coordination to the Lewis acidic lithium due to delocalization of the lone pair of the CH_2 to the vacant p* orbital on lithium. For example, even the interaction of the p* orbital on the CH_2 is weak (IBE = –0.002 a.u.).

Subsequent Reactions. We have investigated the reactions of CH_3OCH_2Li, i.e., the first step of the reaction pathways, starting with the first intermediate involved in the ethylation by methyl ethers in the presence of organometallic bases. The kinetically most favorable reaction was found to be methylene transfer between two molecules of CH_3OCH_2Li, which produces $CH_3OCH_2CH_2Li$. The subsequent reactions are the β-elimination of CH_3OLi from $CH_3OCH_2CH_2Li$ to give ethylene, and finally the insertion of ethylene into the C–Li bond. The two processes were investigated. The second most-favorable initial step is methylene transfer to the carbanionic substrate. This further methylene transfer from CH_3OCH_2Li to the first product CH_3CH_2Li may be involved in the ethylation reaction of our present interest. The reaction is considered to occur with a similar activation energy (27.5 kcal mol^{-1}). The reaction after the third initial reaction, i.e. α-elimination, is the dimerization of methylene. This reaction is already known to occur with no barrier.[17]

β-Elimination of $CH_3OCH_2CH_2Li$. The activation energy of the β-elimination of CH_3OLi from $CH_3OCH_2CH_2Li$ (Eq. 5) is low (5.4 kcal mol^{-1}). The reaction proceeds without any difficulty. We analyzed the electronic feature at the transition state to find the preferred σ bond model (Fig. 12). The transition state is early. An analysis of the bond interaction at the transition state showed strong coordination of the metal to the oxygen and significant delocalization from σ_{C-Li} to σ^*_{C-O} (Fig. 13), as expected.

Insertion of Ethylene into the C–Li Bond. Methyllithium was employed as the most simple substrate (Eq. 6). The barrier is 26.7 kcal mol^{-1} from the methyllithium-ethylene π-complex (Fig. 14). The σ bond model has the highest Lewis index (Fig. 15). The transition state is product-like and late.

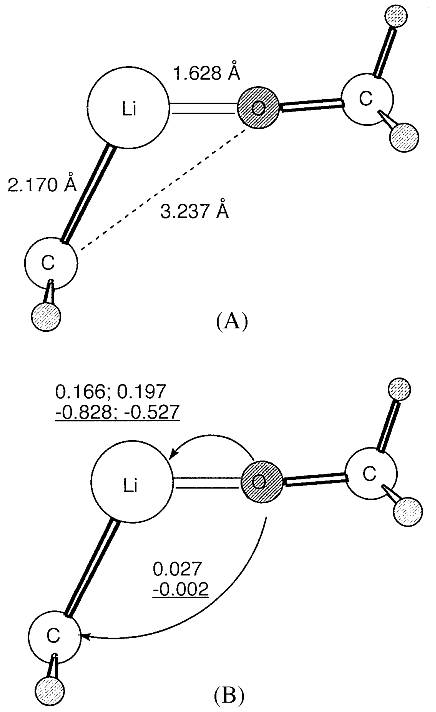

Fig. 10. Transition structure (A) and the delocalization indices and IBE values (underlined) (B) of the carbene formation from CH_3OCH_2Li.

Delocaization between the incipient bonds, or from $\sigma_{C\text{–}Li}$ to $\sigma^*_{C\text{–}C}$ is significant (Delocalization Index = 0.409) among bond-to-bond interactions. The interaction of $\sigma_{C\text{–}C}$ with p^*_{Li} is considerable (Delocalization index = 0.198) (Fig. 16).

Ethylation of CH_3M by CH_3OCH_2M. A possible mechanism of the ethylation reaction of CH_3Li by CH_3OCH_2Li is summarized in Scheme 1. The methylene transfer from CH_3OCH_2Li has been found to prefer CH_3OCH_2Li rather than CH_3Li. This preference comes from an outward extension of the donative $\sigma_{C\text{–}Li}$ of CH_3OCH_2Li, which results from the strong coordination of oxygen atom to the Li, leading to a better overlap with $\sigma^*_{C\text{–}O}$ at the transition state. The results have suggested that the generation of $CH_3OCH_2CH_2Li$, a precursor of ethylene, should occur more readily than direct methylation on the carbanion center of the substrate or sequential methylation leading to products that are shorter or longer than the ethyl group.

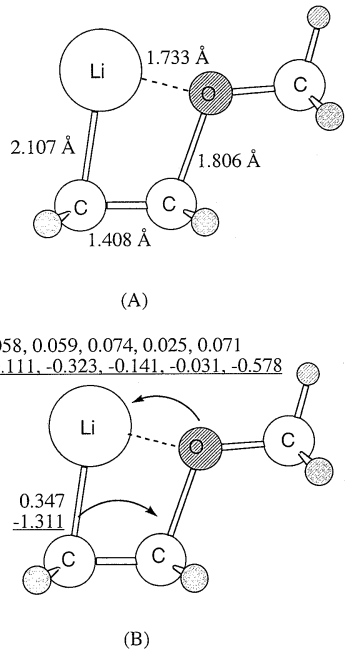

Fig. 13. Transition structure (A) and the delocalization indices and IBE values (underlined) (B) of the β-elimination reaction of methoxyethyllithium.

The calculated activation energies can rule out a reaction pathway via carbene generation from CH_3OCH_2Li by α-elimination followed by insertion to the organometallic *in situ* or its dimerization into ethylene. The activation energy of the carbene generation is higher than that of the methylene transfer

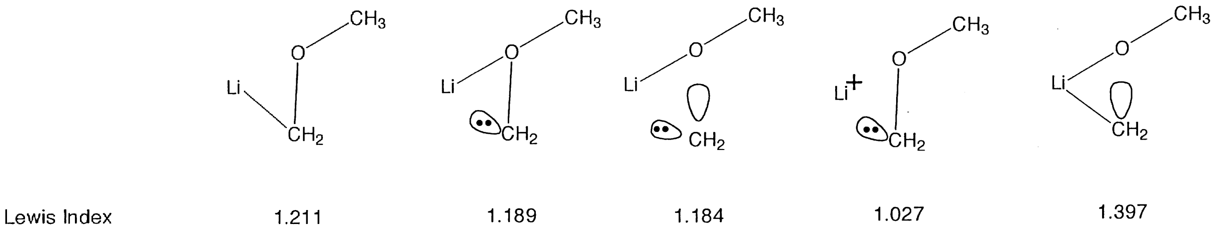

Fig. 11. Lewis Index of the TS of the α-elimination of methoxymethyllithium.

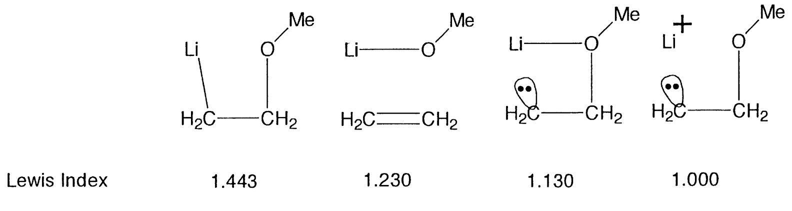

Fig. 12. Lewis Index of the TS of the β-elimination of methoxyethyllithium.

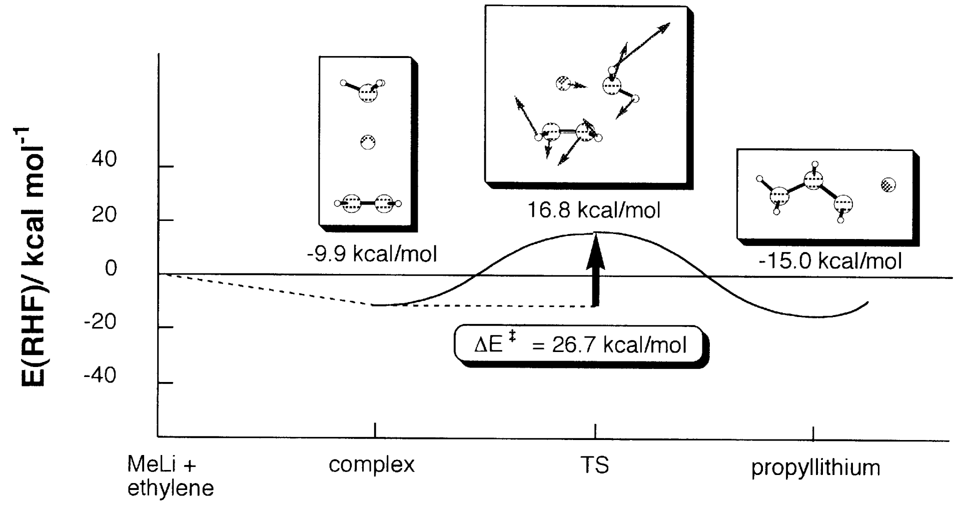

Fig. 14. Reaction profile of addition of MeLi to ethylene.

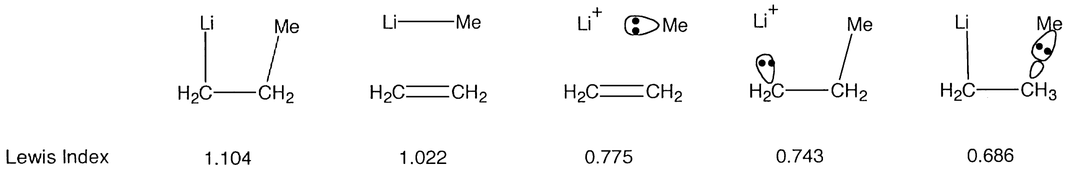

Fig. 15. Lewis Index of the transition state of addition of MeLi to ethylene.

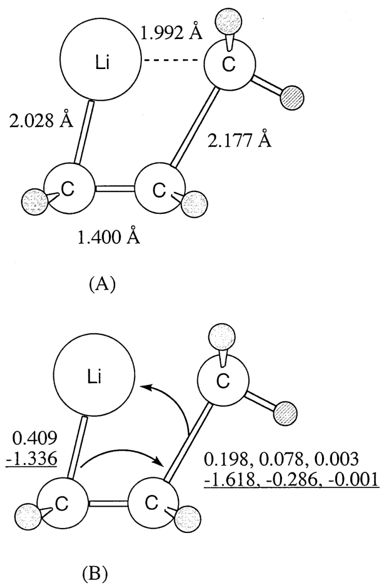

Fig. 16. Transition structure (A) and the delocalization index and IBE value (underlined) (B) of the addition of methyllithium to ethylene.

between two molecules of CH_3OCH_2Li to generate the ethylene precursor, $CH_3OCH_2CH_2Li$. The primary carbanion is reported as being more difficult to react with ethylene than the secondary one.[18] A further ethylene insertion was thus avoided, to obtain the corresponding ethylated product predominantly.

The reactions of butyllithium with dimethyl ether, reported by Ziegler,[3] suggest sequential insertions of methoxymethyllithium or carbene, generated *in situ* from dimethyl ether, to the alkyllithium rather than the predominant ethylation. The reaction conditions are different from each other. We cannot explain the difference in any convincing manner. However, the present work disclosed the significance of potassium species. Ziegler employed only alkyllithium for deprotonation of dimethyl ether. The nucleophilic substitution reactions between two molecules of CH_3OCH_2M to give the precursors of ethylene do not take advantage of the potassium species, which lowers the activation energy. The methylene transfer should considerably compete with ethylene generation. Thus, a mixture of pentane, hexane, heptane, and other normal hydrocarbons was obtained in contrast to our results.

Ethylation of Indole Dianion by Methyl Ethers. We can infer a plausible reaction pathway of the ethylation of the indole dianions by methyl ethers in the presence of organometallic BuLi–*t*-BuOK bases. Alkoxymethylpotassium and -lithium are generated by deprotonation from the methyl ethers. A nucleophilic attack of an alkoxymethylpotassium occurs on an alkoxymethyllithium as an electrophilic substrate to give 2-methoxyethyllithium. 2-Methoxyethyllithium eliminates lithium methoxide, affording ethylene, which reacts with the indole dianion to produce C_2-elongated indoles. The primary carbanion is reported to be difficult to react with ethylene.[18] Further insertion of ethylene was thus avoided.

We examined the reactivities of the other methyl analogs, methyl sulfides and methylamines.[3,12] The key step of the ethylation reactions has been found to be ethylene transfer reactions between two molecules of metallated species, controlled by the interaction of the σ_{C-M} and σ^*_{C-X} bond orbitals. The optimized structures are shown in Fig. 17, which were subjected to bond analyses. The orbital energies are listed in Table 4. The energy gap of CH_3SCH_2Li is smaller than that of CH_3OCH_2Li. However, the bond angle (76.4°) of Li–C–S is wider than that of the Li–C–O in CH_3OCH_2Li. This hinders the effective overlap of σ_{C-Li} with σ^*_{C-S} (Fig. 18). The greater energy gap between the σ_{C-Li} and the σ^*_{C-N} bond orbitals and the wider Li–C–N bond angle (67.6°) both suggest that dimethylaminomethyllithium is less reactive than methoxymethyllithium. In fact, the yields of the ethylated product are lower than 5% for both dimethylsulfide and *t*-buthyldimethylamine.[19]

Conclusion

We have investigated the structures and the reactions of CH_3OCH_2M (M = Li, Na, K). The analysis of the bond interactions in the σ bond model of the highest Lewis index showed that the M–C–O acute angle comes from strong coordination of the oxygen to the metal. The significant O–C–M bending leads to an outward deviation of the bonding orbital from the C–M bond axis (in Fig. 3), which facilitates a nucleophilic attack without any disturbance by the metal atoms. The energy of the bonding orbitals of the C–M bonds increases in the order $\sigma_{C-Li} < \sigma_{C-Na} < \sigma_{C-K}$, as is expected from the ionization potentials of the metals (Table 2), suggesting that the potassium intermediate is the most powerful donor. The most electron-accepting bond orbitals are the antibonding orbitals of the bonds between the oxygen atom and the metallated carbon. The σ^*_{C-O} energy also increases in the same order, suggesting that the lithium derivative is the most powerful electron acceptor.

We have examined the reactions of CH_3OCH_2M, i.e., (a) methylene transfer from one molecule to another to produce $CH_3OCH_2CH_2M$, (b) methylene transfer to CH_3M, and (c) α-elimination to generate methylene, together with the subsequent reactions. The methylene transfer reaction between two molecules was found to occur most readily. The reaction is a nucleophilic substitution where one molecule acts as a nucleophile, while the other molecule acts as an electrophile. The nucleophilic center is the carbon atom bonded to M. The leaving group is the methoxy group. The important interaction takes place between σ_{C-M} in the nucleophilic molecule and σ^*_{C-O} in the electrophilic molecule. The best nucleophile and electrophile are CH_3OCH_2K and CH_3OCH_2Li, respectively, of the CH_3OCH_2M (M = Li, Na, K) examined here. The product $CH_3OCH_2CH_2M$ was found to generate ethylene more readily by elimination.

The present study has supported the postulated mechanism (Scheme 1)[1] for ethylation of the indole derivatives by methyl ethers in the presence of the organometallic base. Methyl

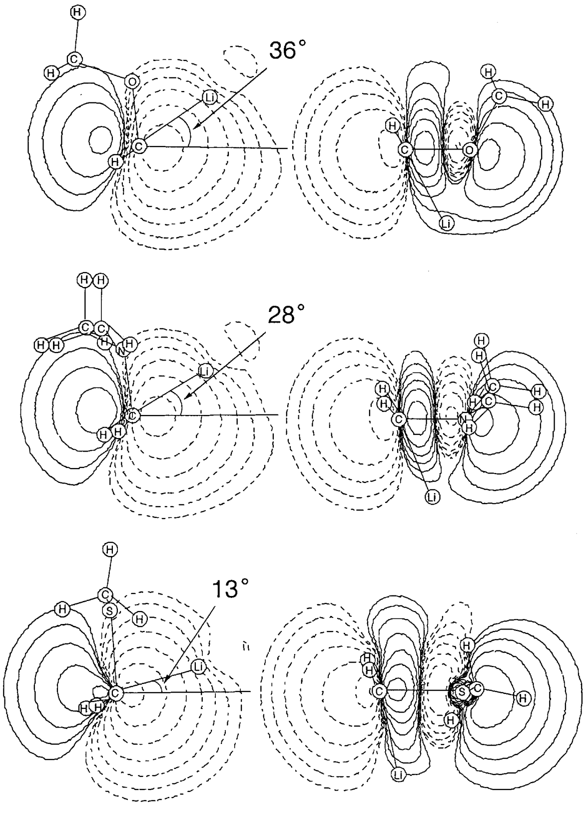

Fig. 18. σ_{C-Li} and σ^*_{C-X} of (a) CH_3OCH_2Li, (b) $(CH_3)_2NCH_2Li$, and (C) CH_3SCH_2Li.

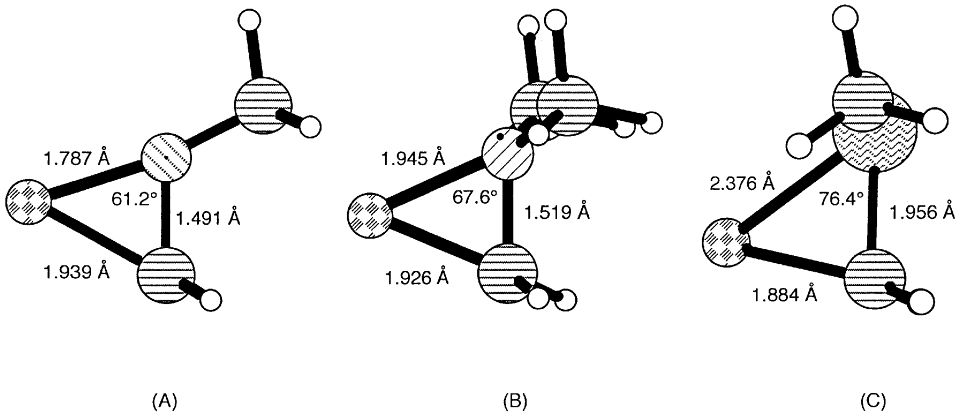

Fig. 17. The optimized structures of (A) CH_3OCH_2Li, (B) $(CH_3)_2NCH_2Li$ and (C) CH_3SCH_2Li.

ethers are transformed into alkoxymethylmetallics, which undergo the nucleophilic substitution between two molecules to afford β-alkoxyethyl metal, a precursor of ethylene. The reactions of ethylene with indole dianions give ethylated indole derivatives after quenching.

This work has been financially supported by a Grant-in-Aid (No. 09750900) from the Ministry of Education, Science, Sports, and Culture, Japan as well as the Research Promotion Fund of Faculty of Engineering, Gifu University.

References

1 Y. Naruse, K. Kido, and S. Inagaki, *J. Org. Chem.*, **60**, 8334 (1995).

2 M. Schlosser, *J. Organomet. Chem.*, **8**, 9 (1967); M. Schlosser, J. H. Choi, and S. Takagishi, *Tetrahedron*, **46**, 5633 (1990). For review: M. Schlosser, in "Modern Synthetic Methods," ed by Scheffold, R., Verlag Helvetica Chimica Acta: Basel, 1992; Vol. 6, pp 227-272; M. Schlosser, in "Organometallics in Synthesis," John Wiley and Sons: Chichester (1994), pp. 1–166.

3 K. Ziegler, and H. G. Gellert, *Liebigs Ann. Chem.*, **567**, 185 (1950). For review: A. Maercker, *Angew. Chem., Int. Ed. Engl.*, **26**, 972 (1987).

4 a) J. Ma and S. Inagaki, *J. Phys Chem. A*, **104**, 8989 (2000). b) The C_G values are previously[4c] termed the Kekulé index to indicate the weights of the Kekulé structure of polycyclic aromatic molecules. c) S. Inagaki and Y. Hirabayashi, *Bull. Chem. Soc. Jpn.*, **51**, 2283 (1978). See also: S. Inagaki, N. Goto, and K. Yoshikawa, *J. Am. Chem. Soc.*, **113**, 7144 (1991); S. Inagaki, K. Yoshikawa, and Y. Hayano, *J. Am. Chem. Soc.*, **115**, 3706 (1993); S. Inagaki, Y. Ishitani, and T. Kakefu, *J. Am. Chem. Soc.*, **116**, 5954 (1994); S. Inagaki, T. Kakefu, T. Yamamoto, and H. Wasada, *J. Phys. Chem.*, **100**, 9615 (1996); K. Iwase, and S. Inagaki, *Chem. Lett.*, **1993**, 1619; K. Iwase, S. Sakai, and S. Inagaki, *Chem. Lett.*, **1994**, 1601; S. Inagaki, S. Ohashi, and T. Kawashima, *Org. Lett.*, **1**, 1145 (1999); S. Inagaki, and S. Ohashi, *Theo. Chem. Acc.*, **102**, 65 (1999).

5 S. Inagaki, H. Kawata, and Y. Hirabayashi, *Bull. Chem. Soc. Jpn.*, **55**, 3724 (1982).

6 K. Iwase, and S. Inagaki, *Bull. Chem. Soc. Jpn.*, **69**, 2781 (1996).

7 S. Inagaki, T. Yamamoto, and S. Ohashi, *Chem. Lett.*, **1997**, 977.

8 S. Inagaki, and Y. Hirabayashi, *Chem. Lett.*, **1982**, 709; S. Inagaki, H. Kawata, and Y. Hirabayashi, *J. Org. Chem.*, **48**, 2928 (1983), S. Inagaki, *Bull. Chem. Soc. Jpn.*, **57**, 3599 (1984); S. Inagaki, K. Iwase, and N. Goto, *J. Chem. Soc., Perkin Trans. 2*, **1984**, 2019; S. Inagaki, K. Iwase, and H. Kawata, *Bull. Chem. Soc. Jpn.*, **58**, 601 (1985); S. Inagaki, K. Iwase, and N. Goto, *J. Org. Chem.*, **51**, 362 (1986); S. Sakai, and S. Inagaki, *J. Am. Chem. Soc.*, **112**, 7961 (1990).

9 a) H. Ikeda, Y. Naruse, and S. Inagaki, *Chem. Lett.*, **1999**, 363. b) S. Inagaki, H. Ikeda, T. Kawashima, *Tetrahedron Lett.*, **40**, 8893 (1999).

10 S. Inagaki, and H. Ikeda, *J. Org. Chem.*, **63**, 7820 (1998).

11 Calculated structures are deposited as Document No. 74016 at the Office of the Editor of Bull. Chem. Soc. Jpn.

12 Gaussian 98, Revision A.7, M. J. Frisch, G. W. Trucks, H. B. Schlegel, G. E. Scuseria, M. A. Robb, J. R. Cheeseman, V. G. Zakrzewski, J. A. Montgomery, Jr., R. E. Stratmann, J. C. Burant, S. Dapprich, J. M. Millam, A. D. Daniels, K. N. Kudin, M. C. Strain, O. Farkas, J. Tomasi, V. Barone, M. Cossi, R. Cammi, B. Mennucci, C. Pomelli, C. Adamo, S. Clifford, J. Ochterski, G. A. Petersson, P. Y. Ayala, Q. Cui, K. Morokuma, D. K. Malick, A. D. Rabuck, K. Raghavachari, J. B. Foresman, J. Cioslowski, J. V. Ortiz, A. G. Baboul, B. B. Stefanov, G. Liu, A. Liashenko, P. Piskorz, I. Komaromi, R. Gomperts, R. L. Martin, D. J. Fox, T. Keith, M. A. Al-Laham, C. Y. Peng, A. Nanayakkara, C. Gonzalez, M. Challacombe, P. M. W. Gill, B. Johnson, W. Chen, M. W. Wong, J. L. Andres, C. Gonzalez, M. Head-Gordon, E. S. Replogle, and J. A. Pople, Gaussian, Inc., Pittsburgh PA, 1998.

13 H. Wasada and Y. Tsutsui, *Bull. Fac. Gen. Edu., Gifu Univ.*, **33**, 145 (1996).

14 P. v. R.Schleyer, T. Clark, A. J. Kos, G. W. Spitznagel, C. Rohde, D, Arad, K. N. Houk, and N. G. Rondan, *J. Am. Chem. Soc.*, **106**, 6467 (1984); T. Clark, P. v. R. Schleyer, K. N. Houk, and N. G. Rondan, *J. Chem. Soc., Chem. Commun.*, **1981**, 579. For review: G. Boche, J. C. W. Lohrenz, and A. Opel, in "Lithium Chemistry: theoretical and experimental overview," A. Sapse and P. v. R. Schleyer ed., John Wiley and Sons: New York (1995), pp. 206-226, and references cited therein.

15 a) Another possible reaction of CH_3OCH_2Li is the Wittig rearrangement to C_2H_5OM. Tonachini[15b] recently reported that the activation energy is high (38.3 kcal mol^{-1}). We did not reinvestigate the reaction in this paper; b) P. Antoniotti, and G. Tonachini, *J. Org. Chem.*, **63**, 9756 (1998).

16 Y. Tanaka, M. Hada, K. Atsushi, K. Tamao, H. Nakatsuji, *Organometallics*, **17**, 4573 (1998). See also: K. Tamao, and A. Kawachi, *Organometallics*, **14**, 3108 (1995); K. Obata, and M. Kira, *Organometallics*, **18**, 2216 (1999).

17 L. M. Cheung, K. R. Sundberg, and K. Ruedenberg, *J. Am. Chem. Soc.*, **100**, 8024 (1978).

18 P. D. Bartlett, S. J. Tauber, and W. P. Weber, *J. Am. Chem.Soc.*, **91**, 6362 (1969); P. D. Bartlett, C. V. Goebel, and W. P. Weber, *J. Am. Chem. Soc.*, **91**, 7425 (1969).

19 Treatment of 1,2,3,4-tetrahydrocarbazole (0.17 g, 1.0 mmol) with freshly distilled dimethyl sulfide or *t*-butyldimethylamine (10 mL) in the presence of BuLi–*t*-BuOK (11 mmol and 10 mmol, respectively) gave 1-ethyl-1,2,3,4-tetrahydrocarbazole only in trace amount (less than 5%), which was detected by GC–MS analyses by comparison with the authentic sample.